# LEAF-MOUNTED MICRONEEDLE-BASED MULTISENSORY PLATFORM FOR MULTIPLEXED MONITORING OF PHYTOHORMONES IN LIVE PLANTS

*Nafize I. Hossain and Shawana Tabassum**
The University of Texas at Tyler, Tyler, TX, USA

## ABSTRACT

This paper presents a first-of-its-kind leaf-mounted microneedle-based multisensory platform for *in situ* monitoring of salicylic acid and indole-3-acetic acid in the leaves of a live plant. The multiplexed system has a built-in temperature sensor for temperature correction. The sensor could accurately detect salicylic acid and indole-3-acetic acid levels with detection limits of 1μM and 0.10μM, respectively. The measured hormone levels were corrected based on the variations in leaf temperature in an actual field condition. Since phytohormone signaling is a plant's first response to environmental stresses, early identification of these stress hormones will help growers to implement site-specific interventions and mitigate productivity losses. Moreover, our continuous and *in situ* sensor will advance future research on improving plant growth in space missions (NASA Space Biology's research priority).

## KEYWORDS

Microneedle sensor, multisensory platform, leaf-wearable sensor, multiplexed monitoring, salicylic acid, indole-3-acetic acid.

## INTRODUCTION

Plants have sophisticated systems to detect and respond to environmental stimuli. Real-time measurement of plant parameters is crucial to gauge the adverse ecological impacts and intervene early. Studies report that drought stress alone yielded 21% and 40% of global reductions in wheat and maize productions, respectively, between 1980 and 2015 [1]. The impacts of these stressors on crop yield are often not detected early enough to mitigate crop damage. Environmental stresses induce a progressive change in the levels of phytohormones, which are circulated throughout the plant via xylem and phloem. Thus, the levels of phytohormones can serve as early signals of plant stress [2-5]. Salicylic acid (SA), jasmonic acid (JA), abscisic acid (ABA), and indole-3-acetic acid (IAA) are among the most important regulators of induced defense mechanisms [6-10]. Progressive variations in their levels have been reported in many drought, salt, and cold/heat-stressed plants. Moreover, exogenous application of these hormones mitigates oxidative stress in plants [11-16]. The interconnected signaling pathways of these hormones are central to the plant's ability to fine-tune the induction of defenses in response to stresses. *However, the dynamic interaction mechanism of these hormones under environmental stress conditions is not fully elucidated due to the lack of knowledge and technology needed to facilitate the use of in situ sensors.*

The traditional approaches to conducting molecular analyses of plants include liquid chromatography (LC), nuclear magnetic resonance (NMR) imaging, and infrared (IR) spectroscopy. Although LC and NMR methods are highly sensitive and selective, they are limited to laboratory settings [17]. In addition, they are non-continuous, disruptive, time-consuming, laborious, and expensive (>$100k): the tissue samples need to be collected in the field and brought to the laboratory periodically and throughout the growing season. Moreover, the collected samples lose their functionality due to the need to transport long distances to the lab. The time lag between sample collection and analysis prevents follow-up and dynamical studies [17]. Due to the complexities and time delays associated with these techniques, only a few plants are sampled, and extrapolations are made about the whole population, thereby neglecting the significant variations between plants across a field. The infrared and thermal imaging techniques provide a non-disruptive view of the action of the stressors in plants. Still, they lack accuracy, do not provide quantitative analysis of metabolites, and are effective only at late crop responses. Unmanned aerial systems have emerged as an attractive tool for aerial scouting. They can fly to waypoints, hover, and collect high-resolution data (millimeters per pixel) from large acres of the field quickly. However, they do not conduct chemical profiling of the plant and are very power-hungry, requiring human intervention for battery recharge/replacement. It can take an entire 8-hours workday to exhaustively collect high-definition images from every zone in an 80-acre crop field [18, 19]. The commercial in-situ crop sensors (e.g., FloraPulse and Dynamax) do not provide real-time and continuous monitoring of stress responses in plants. They only monitor sap water content and do not provide chemical measurements (e.g., metabolite or nutrient), hence stress profiling. To summarize, *none of the traditional/commercial plant monitoring technologies can provide real-time and continuous assessment of stress responses in plants.*

In contrast, our proposed leaf-mounted multisensory platform has competitive advantages over the existing methods through providing continuous and *in situ* monitoring capabilities, multiplexed detection of stress-related hormones, wireless data transfer capability, and energy efficient and low-cost solution, while incurring minimal damage to the plant. The emerging *in situ* leaf sensors are limited to monitoring leaf temperature, humidity, and volatiles [20]. Although some microneedle structures are reported for plants, they are limited to drug delivery or impedance monitoring [20]. Real-time tracking with our proposed sensor will reduce the losses of valuable cash crops, including cannabis, the fifth most valuable crop in the United States behind corn, soybeans, hay, and wheat.

This work addresses the limitations of traditional plant monitoring techniques through:

a. developing a novel leaf-mounted, bioagent-free microneedle-based multisensory platform for multiplexed monitoring of salicylic acid (SA) and indole-3-acetic acid (IAA) in the leaves of a live plant
b. embedding a temperature sensor on the same chip for *in situ* temperature correction of the phytohormone measurements
c. elucidating phytohormone dynamics under water stress.

## DEVICE MANUFACTURING

The entire system is comprised of a leaf-wearable multisensory module and a data logger.

**Formation of the Microneedle Electrodes**

The 2cm x 1cm device was comprised of three-electrode-based electrochemical sensors. Each electrode was made of an array of square-based pyramid-shaped microneedles with a height of 800μm, a base width of 800μm, and each side making a $30^0$ angle with the tip (Fig. 1a). The entire platform was designed with a stereolithography 3D printer using a biocompatible resin. The working electrodes: $WE_{SA}$, $WE_{IAA}$, $WE_{T,}$ and the counter electrode

978-1-940470-04-7/HH2022/$25©2022TRF
DOI 10.31438/trf.hh2022.33

(CE) were coated with graphene ink, while the reference electrode (RE) was covered with Ag/AgCl paste and subsequently cured at 100°C for 60 minutes. Figure 1b illustrates the microscopic images of the fabricated multisensory platform carrying the microneedle electrodes.

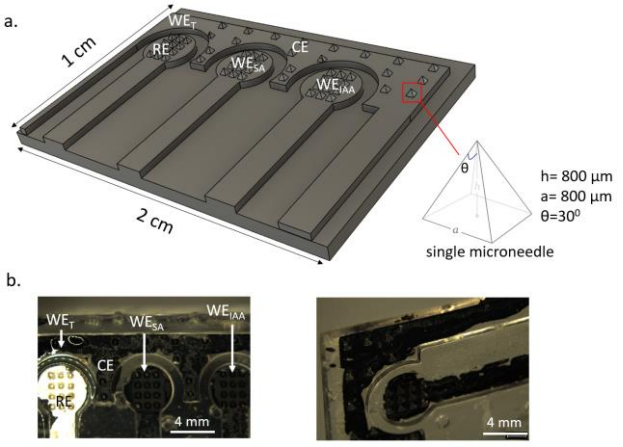


*Figure 1: (a) The microneedle sensor (left) and a single needle (right). (b) Microscopic images (top and side views) of the microneedle sensor.*

**Formation of the Target-Specific Coatings**

The $WE_{SA}$ was coated with a copper-based metal-organic framework (CuMOF) for SA detection [21], $WE_{IAA}$ with gold nanoparticle decorated graphene hydrogel nanocomposite (AuNP-GH) for IAA detection [22], and $WE_T$ with PEDOT:PSS crosslinked by (3-glycidyloxypropyl)trimethoxysilane (GOPS) for temperature detection [23].

Synthesis of the CuMOF coating started by dissolving 0.4 g of polyvinyl pyrrolidone (PVP) in 8 mL of dimethylformamide (DMF) and 8 mL of ethanol. Next, a homogeneous mixture of 46.6 mg of copper nitrate hydride and 10.8 mL of 2-amino terephthalic acid was prepared in 4 mL of DMF, which was added to the previously prepared PVP solution and heated at 100°C for 5 hours. The resulting green residue was dissolved in 40 mL of DMF and heated in an oven at 100°C for 8 hours. The solution was cooled down to room temperature and subsequently centrifuged at 1000 rpm for 30 minutes. The resulting CuMOF precipitates were collected and dried at 100°C. The CuMOF powders were added to carbon black (CB) at a weight ratio of 2:1 and dissolved in deionized water at a 2 mg/mL concentration. After adding 0.01% w/v of Nafion, the solution was sonicated for 30 minutes. Finally, 1 µL of the resulting nanocomposite solution was drop coated on the $WE_{SA}$ electrode surface.

The AuNP-GH was synthesized according to the method described in [22]. Briefly, 1 mg $mL^{-1}$ of graphene oxide suspension was prepared. 20 mL of this suspension was added to 2 mL of 0.8511 mg $mL^{-1}$ chloroauric acid solution and 1 mL of triethylenetetramine. The resulting mixture was sonicated for 10 minutes and then heated at $140^0$C for 12h. The obtained AuNP-GHs were cooled down to room temperature and then freeze-dried for 24 h to form powders that were stored in a desiccator.

To print the temperature sensing layer, 100 mg of PEDOT:PSS solution and 50 mg of non-ionic surfactant Triton X-100 solution (1.3wt% in DI water) were mixed with GOPS (at a GOPS to PEDOT:PSS weight ratio of 9:1). The resulting mixture was centrifuged for 15 min and degassed for 5 min. The solution was drop cast on the working electrode, $WE_T$ (Fig. 1) followed by annealing at 140 °C in air for 30 min to remove the solvent and enable the cross-linking process. Finally, a 25 µm-thick Kapton tape was used as the encapsulation layer to cover the PEDOT:PSS coating.

**Data Logger**

The commercially available handheld EmStat 3 potentiostat (BASi, Inc.) was used to perform the electrochemical measurements of SA and IAA. The onboard temperature sensor was resistive, generating resistance variations in response to varying leaf temperatures. A separate ESP32 feather development board was used to acquire and process the temperature measurements. The temperature sensor was connected in series with a known resistor, and a built-in analog to digital converter on the ESP32 board measured the analog voltages across the sensor. The measured resistance values across the temperature sensor were further verified with a benchtop LCR meter (Applent, AT 3817).

## RESULTS AND DISCUSSION

**Characterization of the Composite Coatings**

The CuMOF coating was characterized by Fourier Transform Infrared (FTIR) spectroscopy, as is demonstrated in Fig. 2a. The FTIR spectrum confirmed the presence of amino groups and -OH and C=O functional groups, also reported in [24]. The AuNP-GH coating was characterized by ultraviolet-visible (UV-Vis) spectroscopy, which indicated the presence of Au molecules and C=O bonds (Fig. 2b).

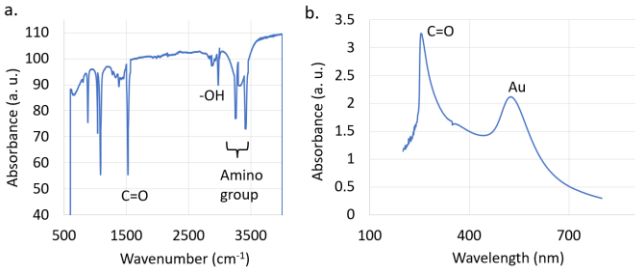


*Figure 2: (a) Characterization of CuMOF coating with FTIR. (b) Characterization of AuNP-GH with UV-Vis.*

**Electrochemical Detection of SA and IAA Hormones**

Differential pulse voltammetry (DPV) was employed for electrochemical measurements of varying SA and IAA levels. The sap was collected from live cabbage plants and spiked with hormones to prepare the SA and IAA concentrations depicted in Fig. 3. In the potential range from -1V to 1.5V, the reduction peak current for CuMOF occurred at around -0.06 V, while the oxidation peak current of SA appeared at 0.82 V (Fig. 3a). Owing to the reasonable separation between the redox potentials, the ratio of the two peak currents was plotted against the SA levels to generate the calibration plot in Fig. 3b. Next, the IAA redox peak current at ~0.85 V (Fig. 3c) was plotted against the IAA concentrations to generate the calibration plot in Fig. 3d. With increasing SA/IAA levels in sap, the redox peak currents for SA/IAA increased due to the oxidation of the hormones by the selective coating. The sensitivity of the SA sensor was calculated as 0.005 $\mu M^{-1}$ with a detection limit of 1 µM. The sensitivity of the IAA sensor was calculated as 0.76149 µA $\mu M^{-1}$ with a detection limit of 0.1 µM.

**Selectivity, Reproducibility, and Repeatability Studies**

The hormone sensors exhibited good selectivity against common interfering species found in sap, as depicted in Fig. 4. The sensors were tested against different interfering species (e.g., Jasmonic acid, L-Cysteine, glucose, citric acid, and ascorbic acid)

and their mixture, commonly found in the plant sap. It was observed that the sensors demonstrated a higher relative signal in response to the target hormones as compared to the interfering species. The relative signal is defined by the following equation [21]:

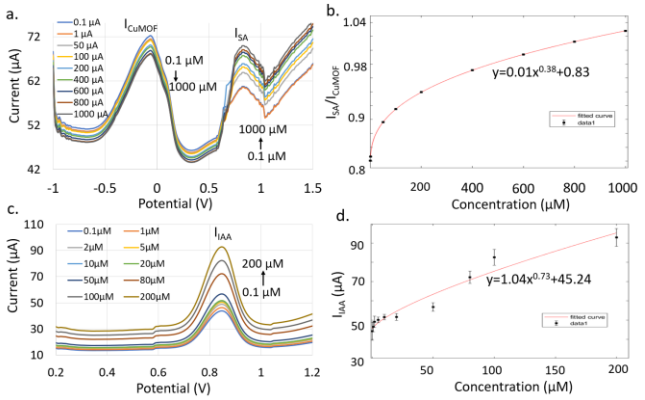


*Figure 3: (a) DPV responses and (b) calibration plot of the SA sensor for varying SA concentrations (sensitivity= 0.005 μM$^{-1}$). (c) DPV responses and (d) calibration plot of the IAA sensor for varying IAA concentrations (sensitivity=0.76149 μA μM$^{-1}$).*

$$Relative\ Signal = (R_a - R_b) / R_b \quad (1)$$

where $R_a$ represents the ratio of the redox peak currents of the analyte and the CuMOF coating. $R_b$ represents the ratio of the base current to the CuMOF peak current of a blank solution.

The hormone sensors also demonstrated excellent reproducibility for 4 repeated measurements with less than 1% deviation (Fig. 5a-b). In addition, with increased temperature, the sensor calibration curves shifted upwards with less than 10% deviation (Fig. 5c-d). Hence, temperature correction was done with an in-built temperature sensor (the results are reported in the next section).

The sensors demonstrated repeatable characteristics under cyclic variations in hormone levels (the same concentrations used for calibration), indicating the feasibility of field deployment (Fig. 5e-f).

**Real-time Hormone Measurements with Temperature Correction**

The microneedle sensor was mounted on the leaf of an unstressed (control) and a water-stressed cabbage plant (Fig. 6a), and SA levels were measured. The stressed plant was not irrigated for three days. The unstressed plant was irrigated 10 hours before the test. Figure 6b shows the calibration plot of the onboard temperature sensor. Figure 6c shows the temperature-corrected real-time SA levels of water-stressed and control plants measured over 7 days with the microneedle sensor. A progressive increase in the SA level was observed in the stressed plant. Next, two sensors were mounted at different heights (0.5 and 6.5 cm) of the same plant. The sensors could accurately measure the SA dynamics across the plant, as was evident from the difference in the SA rise time (3 hours) captured by the leaf sensors (Fig, 6d). The measurements were repeated with three plants and confirmed by the liquid chromatography (LC) tests. As shown in Fig. 6c, the hormone levels measured with the gold standard LC were very close to the levels measured with our sensor, thereby validating the accuracy of the microneedle sensor. Real-time and continuous measurements of hormone levels will advance the research in elucidating the dynamic interaction mechanism of the hormones under environmental stress conditions.

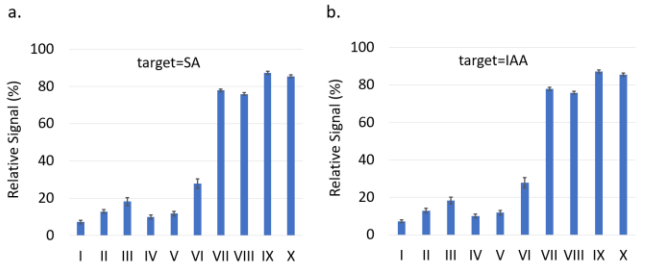


*Figure 4: Selectivity tests of (a) SA and (b) IAA sensors. Here, I -X denote: (I) Jasmonic acid (JA)=50 μM, (II) L-Cysteine (L-Cys)=50 μM, (III) glucose=50 μM, (IV) citric acid=50 μM, (V) ascorbic acid=50 μM, (VI) a mixture of JA, L-Cys, glucose, citric acid, and ascorbic acid (50 μM each), (VII) target hormone=100 μM, (VIII) a mixture of ascorbic acid, JA, L-Cys, glucose, citric acid, ascorbic acid (50 μM each), and target=100 μM, (IX) target (SA=900 μM or IAA=200 μM), (X) a mixture of ascorbic acid, JA, L-Cys, glucose, citric acid, ascorbic acid (50 μM each), and target (SA=900 μM or IAA=200 μM).*

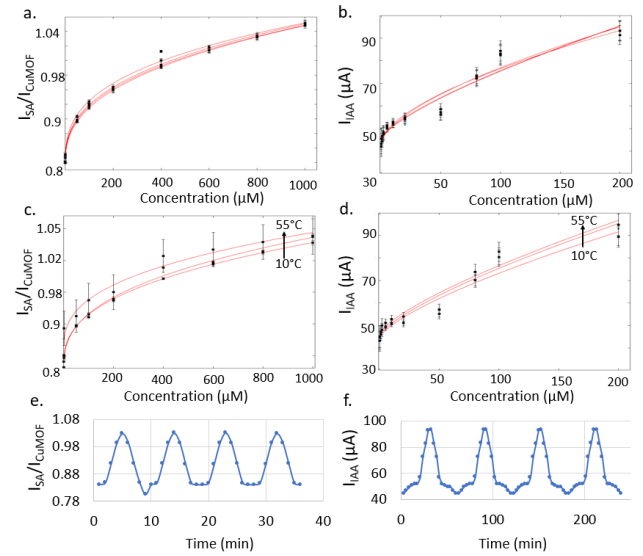


*Figure 5: Reproducibility tests with 4 identical (a) SA and (b) IAA sensors. Shifts in (c) SA and (d) IAA calibration plots for temperature variations (10°C→55°C). Cyclic tests of (e) SA and (f) IAA sensors for different hormone levels.*

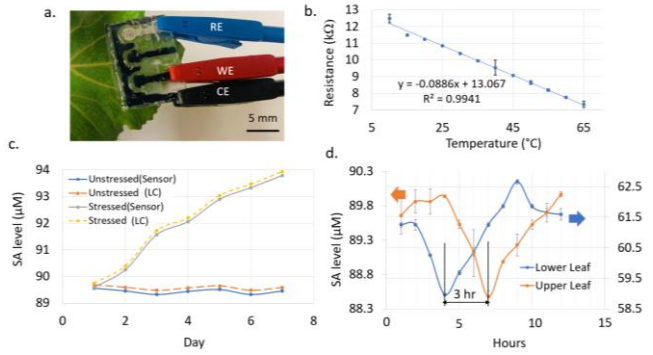


*Figure 6: (a) Optical image of the microneedle sensor mounted on the leaf. (b) Calibration plot of the temperature sensor showed a sensitivity of 0.0886 kΩ/°C. (c) Real-time SA variations in water-stressed vs. control plants for 7 days. Here, LC represents liquid chromatography. (d) SA dynamics over 12 hr, repeated with 3 plants.*

## CONCLUSION

This work reports a leaf-mounted microneedle sensor with temperature correction capability to enable *in situ* and real-time profiling of two potent stress-related phytohormones, which will yield a foundational understanding of dynamic hormonal interactions under environmental conditions and early identification of crop stresses. Real-time crop profiling will help growers implement timely and site-specific applications of agrochemicals to mitigate potential impacts in production. In addition, the results will help guide researchers in the development of plant cultivars with greater stress tolerance. Future work will include the multiplexed detection of other defense-related phytohormones, including methyl jasmonate and abscisic acid.

## ACKNOWLEDGEMENTS

This work was supported by the University of Texas System Board of Regent's Rising STARs award and the University of Texas at Tyler's Internal grant award.

## REFERENCES

[1] S. Fahad, A. A. Bajwa, U. Nazir, S. A. Anjum, A. Farooq, A. Zohaib, S. Sadia, W. Nasim, S. Adkins, S. Saud, M. Z. Ihsan, H. Alharby, C. Wu, D. Wang, and J. Huang, "Crop production under drought and heat stress: plant responses and management options", *Frontiers in Plant Science*, 8, 1147 (2017).

[2] A. R. Seilaniantz, M. Grant, and J. D. G. Jones, "Hormone crosstalk in plant disease and defense: More than just jasmonate-salicylate antagonism", *Annu. Rev. Phytopathol.*, 49, 317–343 (2011).

[3] S. H. Spoel and X. Dong, "How do plants achieve immunity?: Defense without specialized immune cells", *Nature Reviews Immunology*, 12, 89–100 (2012).

[4] J. Yang, G. Duan, C. Li, L.Liu, G. Han, Y. Zhang, and C. Wang, "The crosstalks between Jasmonic acid and other plant hormone signaling highlight the involvement of Jasmonic acid as a core component in plant response to biotic and abiotic stresses", *Frontiers in Plant Sci.*, 10, 1349 (2019).

[5] Z. Q. Fu and X. Dong, "Systemic acquired resistance: Turning local infection into global defense", *Annual Review of Plant Biology*, 64(1), 839–863 (2013).

[6] I. A. Vos, C. M. J. Pieterse, and S. C. M. van Wees, "Costs and benefits of hormone-regulated plant defences", *Plant Pathology*, 62(S1), 43–55 (2013).

[7] L. Philippot, J. M. Raaijmakers, P. Lemanceau, and W. H. van der Putten, "Going back to the roots: the microbial ecology of the rhizosphere", *Nature Reviews Microbiology*, 11, 789–799 (2013).

[8] M. A. Mir, R. John, M. N. Alyemeni, P. Alam, and P. Ahmad, "Jasmonic acid ameliorates alkaline stress by improving growth performance, ascorbate glutathione cycle and glyoxylase system in maize seedlings", *Scientific Reports*, 8, 2831 (2018).

[9] R. Bari and J. D. G. Jones, "Role of plant hormones in plant defense responses", *Plant Mol. Biol.*, 69, 473–488 (2009).

[10] B. N. Kunkel and C. P. Harper, "The roles of auxin during interactions between bacterial plant pathogens and their hosts", *J. Experimental Botany*, 69, 245–254 (2018).

[11] N. Saruhan, A. Saglam, A. Kadioglu, "Salicylic acid pretreatment induces drought tolerance and delays leaf rolling by inducing antioxidant systems in maize genotypes", *Acta Physiol. Plant*, 34, 97–106 (2012).

[12] A. H. Elhakem, "Salicylic acid ameliorates salinity tolerance in maize by regulation of phytohormones and osmolytes", *Plant, Soil and Environment,* 66, 533–541 (2020).

[13] A. A. H. A. Latef, A. Akter, and Md. T. Ul-Arif, "Foliar application of auxin or cytokinin can confer salinity stress tolerance in Vicia faba L", *Agronomy*, 11, 790 (2021).

[14] M. Sharma and A. Laxmi, "Jasmonates: emerging players in controlling temperature stress tolerance", *Frontiers in Plant Sci.*, 6, 1129 (2015).

[15] G. Li, C. Zhang, G. Zhang, W. Fu, B. Feng, T. Chen, S. Peng, L. Tao, and G. Fu, "Abscisic acid negatively modulates heat tolerance in rolled leaf rice by increasing leaf temperature and regulating energy homeostasis", *Rice*, 13, 18 (2020).

[16] Agnieszka Bielach, Monika Hrtyan, and Vanesa B. Tognetti, "Plants under stress: involvement of auxin and cytokinin", *Int. J. Mol. Sci.*, 18(7), 1427 (2017).

[17] A. Galieni, N. D'Ascenzo, F. Stagnari, G. Pagnani, Q. Xie, and M. Pisante, "Past and future of plant stress detection: an overview from remote sensing to positron emission tomography", *Frontiers in Plant Sci.*, 11, 609155 (2021).

[18] Z. Zhang, J. Boubin, C. Stewart, and S. Khanal, "Whole-field reinforcement learning: a fully autonomous aerial scouting method for precision agriculture", *Sensors*, 20, 6585 (2020).

[19] J. Cerro, C. C. Ulloa, A. Barrientos, and J. de L. Rivas, "Unmanned aerial vehicles in agriculture: a survey", *Agronomy*, 11, 203 (2021).

[20] H. Yin, Y. Cao, B. Marelli, X. Zeng, A. J. Mason, C. Cao, "Soil sensors and plant wearables for smart and precision agriculture," *Adv. Mat.*, 33 (2021).

[21] N. I. Hossain, T. Noushin and S. Tabassum, "Leaf-FIT: A Wearable Leaf Sensor for In-Situ and Real-Time Monitoring of Plant Phytohormones", Proceedings of the *2021 IEEE Sensors*, pp. 1-4, doi: 10.1109/SENSORS47087.2021.9639842.

[22] X. Cao, X. Zhu, S. He, X. Xu, Y. Ye, and S. Gunasekaran, "Gold nanoparticle-doped three-dimensional reduced graphene hydrogel modified electrodes for amperometric determination of indole-3-acetic acid and salicylic acid", *Nanoscale*, 11, 10247-10256 (2019).

[23] Y. -F. Wang, T. Sekine, Y. Takeda, K. Yokosawa, H. Matsui, D. Kumaki, T. Shiba, T. Nishikawa, and S. Tokito, "Fully printed PEDOT:PSS-based temperature sensor with high humidity stability for wireless healthcare monitoring", *Sci. Rep.*, 10, 2467 (2020).

[24] S. Wang, W. Deng, L. Yang, Y. Tan, Q. Xie, and S. Yao, "Copper-based metal-organic framework nanoparticles with peroxidase-like activity for sensitive colorimetric detection of staphylococcus aureus", *ACS Appl. Mater. Interfaces*, 29, 24440–24445 (2017).

## CONTACT

*S. Tabassum; stabassum@uttyler.edu